ISSN 1018-5593

European Commission

nuclear science and technology

OKLO Working Group

Proceedings of the third joint EC-CEA progress meeting held in Brussels on 11 and 12 October 1993

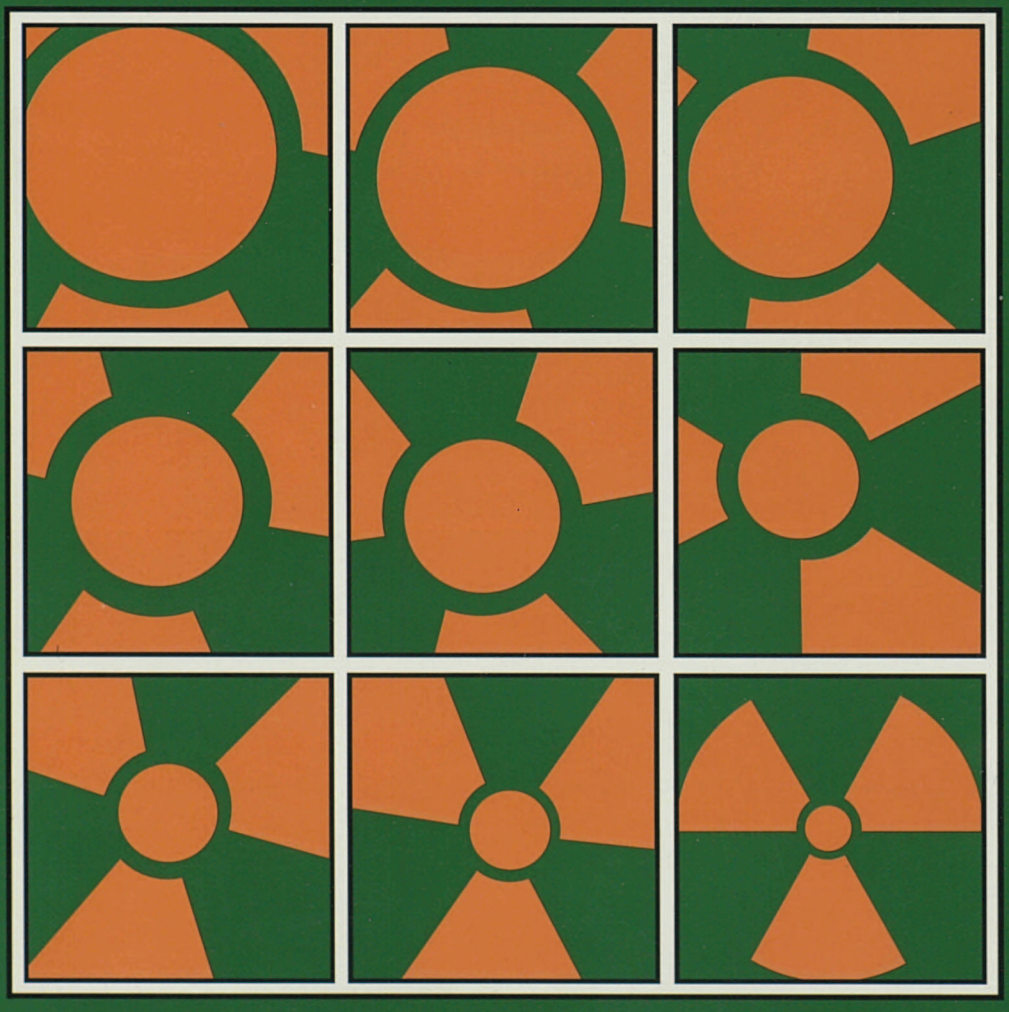

Report

EUR 16098 EN/FR

European Commission

nuclear science and technology

OKLO Working Group

Proceedings of the third joint EC-CEA progress meeting held in Brussels on 11 and 12 October 1993

Edited by
H. von Maravic

European Commission
Rue de la Loi 200
B-1049 Brussels

R&D programme on management and storage of radioactive waste

Directorate-General
Science, Research and Development

1995

EUR 16098 EN/FR

Cataloguing data can be found at the end of this publication

Luxembourg: Office for Official Publications of the European Communities, 1995

ISBN 92-827-0149-2

Printed in Luxembourg

FOREWORD

Natural Analogue studies have been carried out for several years in the frame of the European Community's R&D programme on radioactive waste and within its recent 4th five-year programme on "Management and Storage of Radioactive Waste (1990-1994)" the Community is participating in the Oklo study, natural analogue for radionuclide transport processes in a geological repository.

The Oklo project (covering the research period from 1991 to 1994) is coordinated by CEA-IPSN (F) and involves laboratories from several CEA directorates (IPSN, DTA and DCC) which collaborate with other institutions from France: CREGU, Nancy; CNRS, Strasbourg and EMP, Fontainebleau. Under the umbrella of the 'Oklo Working Group', collaboration has been established with institutions from Canada, Japan, USA and Sweden that are taking part in the study.

The 3rd joint CEC-CEA progress meeting of the 'Oklo Working Group' was held on 11-12 October 1993 in Brussels and gave the possibility of reviewing and discussing progress made since its 2nd meeting in April 1992 in Brussels. The meeting focused on the different tasks within the CEC-CEA Oklo project and further research activities of the other participants in the Oklo study concerning (i) field survey and in-situ sampling, (ii) characterisation of the source term, (iii) studies of the petrographical and geochemical system ruling the ancient and recent migration system and (iv) integration of hydrogeological and hydrochemical data into a coupled flow and transport model.

Implications of the potential role of the Oklo Natural Analogues studies to be used in repository performance assessment has also been presented and discussed by considering methodological aspects, geochemical transport mechanisms and waste disposal aspects.

The proceedings present the papers presented at the third progress meeting of the 'Oklo Working Group'. A first progress report was published in 1993 under EUR 14877 EN.

H. von Maravic
(CEC)

P.L. Blanc
(CEA-IPSN)

SOURCE TERM CHARACTERIZATION : MAIN ISOTOPIC FEATURES AND MODELLING OF REACTOR ZONES 10 & 13

Philippe HOLLIGER
DESD/ SCS/ LGCA, CEA Cadarache

1- Objective and scope

This part of the programme is specially aimed at characterizing reactor cores 10 and 13 (so called "source term") at Oklo. The isotopic compositions and abundances of uranium and fission products presently found in these two reactor zones (R.Z.) enable us: - to calculate the nuclear parameters from fission reactions [1] and - to compare the two types of reactors located near to a 20 meters-wide dolerite dike intrusion which has affected the distribution of U, Pb and fissiogenic isotopes. At Oklo, the geochemical behaviour of radionuclides during fission reactions was closely dependent on mineralogical assemblages from the reactor core and its vicinity and the capabilities for neoformed minerals to retain fission products (F.P.) which would escape from uraninite structure.

Ion microprobe analyses of individual uraninite grains and galenas from reactor core 13 show that radiogenic lead was completely lost from uraninite and permit us to calculate an indirect U-Pb age of about 800-900 Ma for the dolerite intrusion (c.f. §.3.2). The petrography of this reactor core was drastically modified by the hydrothermal activity related to this intrusion: uraninite was restructured; galena and neoformed minerals then crystallised. The U-Pb datings performed on R.Z.10 (this zone is located 70-80 meters away from the dike) indicate that a Pb loss also occured in some places of the R.Z., about 850 Ma ago. However, uraninites embedded in organic matter and in resilicified rocks within the reactor core, have given an age of 1970 Ma in good agreement with that calculated by Naudet from F.P. [2].

Based - on topographic coordinates and petrographic descriptions of galleries and drill-holes mined mainly during the period 1989-1992 (this contract) and - on a compilation of ratios $^{235}U/^{238}U$ available to-day, a 3D simple geological model is proposed for the reconstruction of R.Z.10.

2- Topography and modelling of R.Z.10

The modelling study of R.Z.10 consists of a geometric plot of structural data (geological model) available for describing the different layers of the R.Z and a 3D reconstruction of ^{235}U-isodepleted volumes in order to calculate the total amount of ^{235}U consumed during the criticality of reactor 10.

2.1. Topography of R.Z.10

The first petrographic descriptions and isotope measurements of uranium and F.P. from R.Z.10 were carrried out on borehole SF.29 samples [3-6] in the lower part of zone 10. On the period 1989-1992, a series of galleries and boreholes were mined through the R.Z.; a large number of uranium isotopic measurements were obtained [7-9]. The last sampling was performed in february and march 1992 on organic-rich U-ore crosscuts from gallery D.81N [9]. A topographic view of the envelope of R.Z.10 is shown on Fig.1: it is situated between 120 and 146 m of altitude (z) and it consists of a 1m thick lens covering an area of about 40 m in length x 10-20 m in width [10].

The methodology used for a 3D vision of the R.Z. is described in [10]; all the data were compiled in the "Earth Vision" program developed by the EOSYS company. Four

geological markers, corresponding to stratigraphic levels for the uranium mineralized layer were defined: A and B for the bottom and the top of "faciès-pile" layer respectively, C for Fa U-rich sanstones basal formation and D for Fb black shales basal formation. A 3D view of 122 topographic points from R.Z.10 and the geological model are shown in Fig.2 and 3 respectively. Fig.4 represents the upper limit of Fa sandstones layer and Fig.5 a West-East cross-section of R.Z.10. They show that:
- the "faciès-pile" is continuously present as a lens orientated SE-NW,
- the large deformation of the sandstone layer witnesses to the desilicification of sandstones by hydrothermal circulations during fission reactions (fig.4)
- the compaction of the argilite and pelite layers (level D) at the contact with R.Z.
- a pinching affecting the sandstone layer in the area of boreholes SF.40, SF.42 and SF.83 is observed which could correspond to a fault at level z=140; this induced an increasing of the thickness of the "faciès-pile" layer in the down part of the R.Z.

2.2. $^{235}U/^{238}U$ modelling

53 values of uranium isotopic compositions from R.Z.10 samples [10] were introduced in the "Earth Vision" program. The data on D.81N samples were recently acquired and are not yet taken into account for this modelling. The 3D "Earth Vision" interpolator correlates and adjusts isosurfaces relative to ^{235}U depleted points. The calculations of ^{235}U-isosurfaces were done assuming a congruent case where stratigraphy plays a prominent role (more realistic than the isotropic case where stratigraphy is ignored); this case is suitable to represent e.g. fluid circulations with the stratigraphic layers constraints (sandstones, black shales).

The ^{235}U-isodepleted model illustrated in Fig.6 and 7 show that:
- Fa sandstones are ^{235}U-depleted in the vicinity of borehole SF.30,
- U-rich sandstones from borehole SF.29 have recorded the most depleted ^{235}U values (<0.5%),
- Fb pelite layer was not affected by fission reactions.

After calculating from the interpolator, the volumes of U-rich rocks involved relative to ^{235}U-isodepletion are the followings:
- Case (a) : 12 m^3 for $^{235}U/^{238}U$ values $\leq$ 0.575%
- Case (b) : 80 m^3 for $^{235}U/^{238}U$ values $\leq$ 0.600%
- Case (c) : 310 m^3 for $^{235}U/^{238}U$ values $\leq$ 0.650%
- Case (d) : 1400 m^3 for $^{235}U/^{238}U$ values $\leq$ 0.675%
- Case (e) : 5500 m^3 for $^{235}U/^{238}U$ values $\leq$ 0.700%

Assuming for case (b) a rock density of 4 and a U content of 10% (representative of reactor core), one can calculate that 40 kg of ^{235}U was consumed in the reactor core during the fission reactions. Assuming for case (e) a rock density of 3.1 and U contents of 2% (Faciès-pile and U-rich sandstones), a total of about 90 kg of ^{235}U was burnt. This value is in good agreement with the amount of ^{235}U extracted from this zone (about 40% of the total) and corresponding to about 30 kg.

2.3. Conclusion and future developments

In order to obtain a better precision on the 3D model, the knowledge of a number of parameters has to be improved on such as complementary U isotope data (mainly from galleries D.73 and D.81N), radiometric measurements of crosscuts and walls from galleries and detailed petrographic descriptions (clay minerals occurence).

To date, this 3D modelling of R.Z.10 provides a good starting point for calculating: - the total amount of ^{235}U consumed, - the general balance of fissiogenic isotopes - and the energy liberated from the fission reactions. From this, a convective heat transfer and mass transfer model, taking into account of neoformed minerals and the temperatures recorded [11] in the R.Z., could be elaborated. It would offer the possibility to show the main pathways of hot convective fluids in a real 3D geological modelling.

3- Characteristics of R.Z.13

3.1. Sampling

A series of ten samples used for this study was taken from a drill-hole in gallery SD.37, cross-cutting reactor core 13 (Fig.8). The "faciès-pile" with uranium oxide grains embedded in a clay gangue, as observed in reactor 10, is here totally absent and was probably removed by hydrothermal fluids in relation to dolerite intrusion. The reaction zone consists of a compact lens of very rich uranium ore located between Fa sandstone and Fb pelite layers; it is a 35 cm thick layer of uraninite cemented by clay, calcite, sulphide and exotic minerals. At the top of reactor is located a thin layer (2 cm) composed of millimetric crystals of galena and pyrite embbeded in a clay gangue.The average concentration of UO_2 in these samples is 75% in weight with an average ^{235}U abundance of 0.50%. At a distance of 53 centimeters from the beginning of borehole (sample noted 53), ^{235}U content is depleted down to a value of 0.375%.

3.2. SD.37-S2 borehole : isotopic measurements

Lead and uranium isotopic compositions together with Pb/U, Th/U, Nd/U and Sm/U contents were determined with the ion microprobe. The average of $^{207}Pb/^{206}Pb$ radiogenic ratios (except sample 70) corrected for ^{235}U depletion (Fig.9), corresponds to a Pb-Pb age of 870 ± 40 Ma (2σ precision) for the restructuration of uraninite while Pb/U ratios give an average for chemical age of 480 ± 30 Ma (2σ). The Pb-Pb age is in good agreement with the age assumed for the dolerite dyke intrusion. ^{232}Th derived from ^{236}U formed by neutron capture of ^{235}U, is abundant in reactor core (except sample 55) and its daughter ^{208}Pb has almost the same behaviour.

The isotopic compositions of fission products presently found in the reactor core (especially REEs) and their contents relative to uranium, allow us to evaluate the neutronic and nuclear parameters of the reactor [10,12]. Table 1 gives the main parameters of the reactor core deduced from individual isotopic measurements of $^{235}U/^{238}U$, $^{144}Nd/^{143}Nd$ and $^{148}Sm/^{147}Sm$ and quantitative analyses of (^{143}Nd+ $^{144}Nd)/^{238}U$ and $^{147}Sm/^{238}U$ (Fig.10): the integrated neutron flux (fluence) is high and around 10^{21} n/cm^2 (Fig.11), the restitution factor C (fraction of ^{235}U regenerated by α decay of ^{239}Pu) is relatively low in the center of reactor core (around 0.3), the P.F. age of the reactions is deduced from Nf/U (the total number of fissions per atom of actual ^{238}U). The value of Nf/U in the reactor core is almost constant, around 2.5% (Fig.11) corresponding to a P.F. age of 2.1 Ga, in good agreement with the U-Pb age of reactor criticality. This gives the proof that Nd and Sm formed by fission were effectively retained in uraninite, even after the migration of radiogenic lead occured.

3.3. Imaging SIMS: heterogeneous distributions of F.P.

Imaging SIMS studies of reactor core samples show, locally, a good retention of numerous FP (e.g Rare Earth Elements) and transuranium elements such as ^{236}U and ^{237}Np (to-day, visible through stable isotopes ^{208}Pb, ^{209}Bi) and the existence of tiny inclusions containing Ru, (Tc), Rh, Pd, Mo and Te together with Pb, As and S [13]. Microphases of aluminous phosphate minerals with high amounts of fissiogenic REE are also abundant at the uraninite grains boundaries, in the reactor core (Fig.12). Ion maps of fissiogenic ^{139}La (ion LaO^+) and ^{143}Nd (ion NdO^+) show that lanthanium entirely migrated out of the uraninite lattice whereas neodymium is still present in uraninite. Quantitative analyses carried out on these aluminous phosphates allow us to classify them in the "crandallite group". They could derive from the weathering of preexisting organic

matter (rich in P and S), clay and apatite mineral phases, under grounwaters alteration (dolerite episode or supergene alteration). The crystallization of these neoformed minerals is accompanied by a high chemical fractionation between La (present as a major element) and Sm (as a trace element) that occured during the leaching of hydrothermal groudwaters.

4- Whole-rock samples analyses.

In order to obtain nuclear and geochemical informations in a given volume of reactor core, isotopic and chemical analyses were performed on whole-rock samples. The whole-rock sample consists of the assemblage of minerals present in the R.Z. (uraninite, organic matter, clay minerals, phosphates, ...) ; the geochemical behaviour of radionuclides is closely depending upon this mineralogical assemblage during and after criticality. Table 2 gives the main nuclear characteristics derived from thermal ionisation mass spectrometry analyses (TIMS) on whole-rock powdered samples from R.Z.2, 7-9, 10, 13, Okelobondo and Bangombé [4,8,12]. It appears that Nf/U (and correlated F.P. age) calculations from Nd and Sm are systematically higher for Sm. The REE fractionation is enhanced between La and Sm; on Fig.13, Nf/U measured for La, Ce, Nd and Sm on samples from reactor cores 10, 13 and Bangombé show that a large depletion of La exists in reactor core 13, if compared to R.Z.10 and Bangombé data. It indicates that a massive loss of lanthanium occured out of uraninite during the weathering episode, the crystallisation of neoformed aluminous phosphates retaining only 30% of the total fissiogenic La (Nf/U for Sm is 2.7% and less than 1% for La).

5- Conclusion

The isotopic measurements performed on R.Z. samples, both by SIMS for in situ analyses and TIMS for whole-rocks analyses, have permitted us to explore in detail the geochemical behaviour of FP, uranium, transuranium and associated daughters derived from the fission process. This study shows that the retention of a large part of FP was achieved naturally within ^{235}U-depleted uraninite grains and phase assemblages from reactor core; the existence of neoformed minerals in the R.Z. is closely depending upon microscale conditions of pressure, temperature and chemical conditions when reactors operated. A geological model for heat and mass transfer in R.Z.10 and its vicinity could offer the possibility to represent the localized conditions during criticality; a mass balance of FP coupled with in-situ studies (SIMS, mineralogical and physical properties of the R.Z.) in different portions of the reactor, would provide invaluable information about the long term ability of spent fuel to retain specific elements involved in the fission process in geological media.

References

[1] HOLLIGER P. (1992), Geochemical and isotopic characterization of the Oklo reactor zones (uranium, transuranium, lead and fission products). in Proceedings Joint Commission of the European Communities - Commissariat à l'Energie Atomique, Brussels 6-7 april 1992, EUR Series, 27-38.

[2] NAUDET R. (1991), Oklo : des réacteurs nucléaires fossiles, éd. CEA, Eyrolles, Paris, 1991, 685 pages.

[3] GAUTHIER-LAFAYE F. (1988), Etude pétrographique des sondages SF.29 et SF.42 de la zone de réaction 10. Intérêts de la zone 10 comme analogue naturel. Internal Report, CNRS Strasbourg, déc. 1988, 29 pages.

[4] BROS R., GAUTHIER-LAFAYE F. et STILLE P. (1990), Etude pétrographique et géochimique des argiles associées au réacteur 10 et hors réacteurs. Rapport préliminaire, programme "OKLO-Analogues Naturels", Nov. 1990.

[5] BROS R., GAUTHIER-LAFAYE F. et STILLE P. (1991), Pétrographique et géochimie isotopique des argiles associées au réacteur 10 d'Oklo et à la diagenèse du Francevillien. Rapport de fin de contrat, programme "OKLO-Analogues Naturels", Décembre 1991.

[6] HOLLIGER P. (1991), Systématique U-Pb et Etude isotopique in-situ U - Produits de fission de la zone de réaction hybride SF.29 (zone 10). Autres zones d'intérêt sur le site d'Oklo pour les études futures, Note Technique DEM n°18/91, CEA-CENG, 50 p.,39 fig.,5 pl.

[7] MENET-DRESSAYRE C. (1992), Etude du comportement géochimique des radioéléments et de leurs descendants autour des réacteurs naturels 10 et 13 d'Oklo (Gabon) - Application au stockage des déchets de haute activité. Thesis Univ. Paris XI-Orsay, 12 Octobre 1992.

[8] HIDAKA H., HOLLIGER P. and MASUDA A. (1993), Evidence of fissiogenic Cs estimated from Ba isotopic deviations in a Oklo natural reactor zone. Earth and Planet. Sci. Lett., 114, 391-396.

[9] HOLLIGER P. and LANDAIS P. (1993), Organic matter and uraninite from the Oklo natural fission reactors - Natural analogue of radioactive bitumen and UO2 irradiated fuel. CEC contract, Ann. Report 1992, DSD-93-84, 29 p. + 8 pl.

[10] HOLLIGER P. (1993), Oklo - terme source : paramètres nucléaires. Etude isotopique et topographie de la zone de réaction 10. Rapport Technique DESD n° 93-96, CEA Cadarache, 39 pages.

[11] SAVARY V. et PAGEL M. (1993), Détermination de l'histoire thermique et chimique dans et autour des zones de réactions nucléaires naturelles du gisement d'Oklo (Gabon). Contrat CCE - CEA- CREGU, Rapport annuel 1993.

[12] HIDAKA H. and HOLLIGER P. (1993), REE geochemistry of Oklo and Bangombé natural reactors. Joint Commission of the European Communities - Commissariat à l'Energie Atomique, Brussels 11-12 october 1993, EUR Series, these Proceedings.

[13] HOLLIGER P. (1992), Les nouvelles zones de réaction d'Oklo: datation U-Pb et caractérisation in-situ des produits de fission à l'analyseur ionique."OKLO-Analogues Naturels" Project, Annual Report, Note technique CEN. Grenoble/ DEM n°01/92, 42 p.

Table 1 - Nuclear parameters derived from quantitative isotopic analyses of SD.37-S2 drill-hole, Oklo reactor core 13

Sample	235/238 (% atom)	(143+144)/238 (ppm atom)	147/238 (ppm at.)	FLUENCE ($x10\ n^{21}/cm^2$)	C	Nf/U (%) Nd	Nf/U (%) Sm	Age (10^9 yr) Nd	Age (10^9 yr) Sm
35	0.616	1235	125	0.81	0.68	1.10	0.59	1.3	0.7
45	0.495	2640	460	0.88	0.32	2.34	2.15	2.1	2.0
46	0.490	2705	415	0.90	0.32	2.40	1.95	2.1	1.9
50	0.430	3325	645	1.06	0.23	2.95	3.00	2.2	2.2
53	0.375	2685	525	1.04	0.02	2.38	2.44	2.1	2.1
55	0.446	2675	510	1.04	0.28	2.37	2.39	2.0	2.0
58	0.490	3170	580	1.02	0.40	2.81	2.70	2.1	2.1
63	0.510	3145	535	0.92	0.40	2.79	2.49	2.2	2.1
68	0.498	3310	580	0.96	0.39	2.94	2.70	2.2	2.2
69	0.585	3055	415	0.83	0.59	2.70	1.95	2.2	1.9
69.5	0.585	2500	335	0.76	0.59	2.21	1.57	2.1	1.8
70	0.600	8470	1225	0.74	0.59	7.50	5.70	3.4	3.1

Table 2 - Main nuclear parameters derived from isotopic and chemical analyses of different reactor zones samples

Sample (zone)	235/238 (%)	U (% w.)	TAU ($x10^{21}$)	C	R	Nf/U (%) Nd	Nf/U (%) Sm	Age (10^9 years) Nd	Age (10^9 years) Sm
1/ Whole-rock samples									
KN.50-3548 (2)	0.4650	55.2	1.362	0.490	0.183	3.25	3.46	2.05	2.11
GL.2481 (7)	0.6780	41.0	0.225	0.529	0.171	0.51	0.54	1.82	1.86
GL.3046 (8)	0.5980	28.0	0.486	0.382	0.126	1.19	1.31	1.95	2.05
KP1-2898 (9)	0.6680	2.06	0.531	0.750	0.161	1.50	1.60	2.04	2.10
KP1-2901 "	0.5778	10.5	0.608	0.417	0.239	-	-	-	-
SF84-1469 (10)	0.6048	17.2	0.525	0.460	0.181	1.63	1.64	2.19	2.20
SF84-1480 "	0.5069	7.06	0.798	0.304	0.111	1.59	1.38	1.83	1.68
SF84-1485 "	0.5649	14.9	0.622	0.376	0.140	1.97	1.85	2.25	2.18
SF84-1492 "	0.5797	24.3	0.564	0.382	0.155	1.85	1.90	2.27	2.29
SD37/CD (13)	0.4630	59.4	0.780	0.111	0.241	1.55	2.64	1.86	2.40
OK.84 bis -2724 (Okelobondo)	0.6820	0.38	0.329	0.701	0.145	20.0	16.7	5.15	4.96
BA145-1160	0.6552	45.0	0.308	0.484	0.196	0.83	0.92	2.01	2.10
2/ Clay minerals									
SF29-8534 (10)	0.6709	0.577	0.443	0.719	0.179	0.98	1.09	1.80	1.90
SF29-8553 "	0.6579	0.0069	0.478	0.676	0.113	10.1	15.3	4.10	4.52

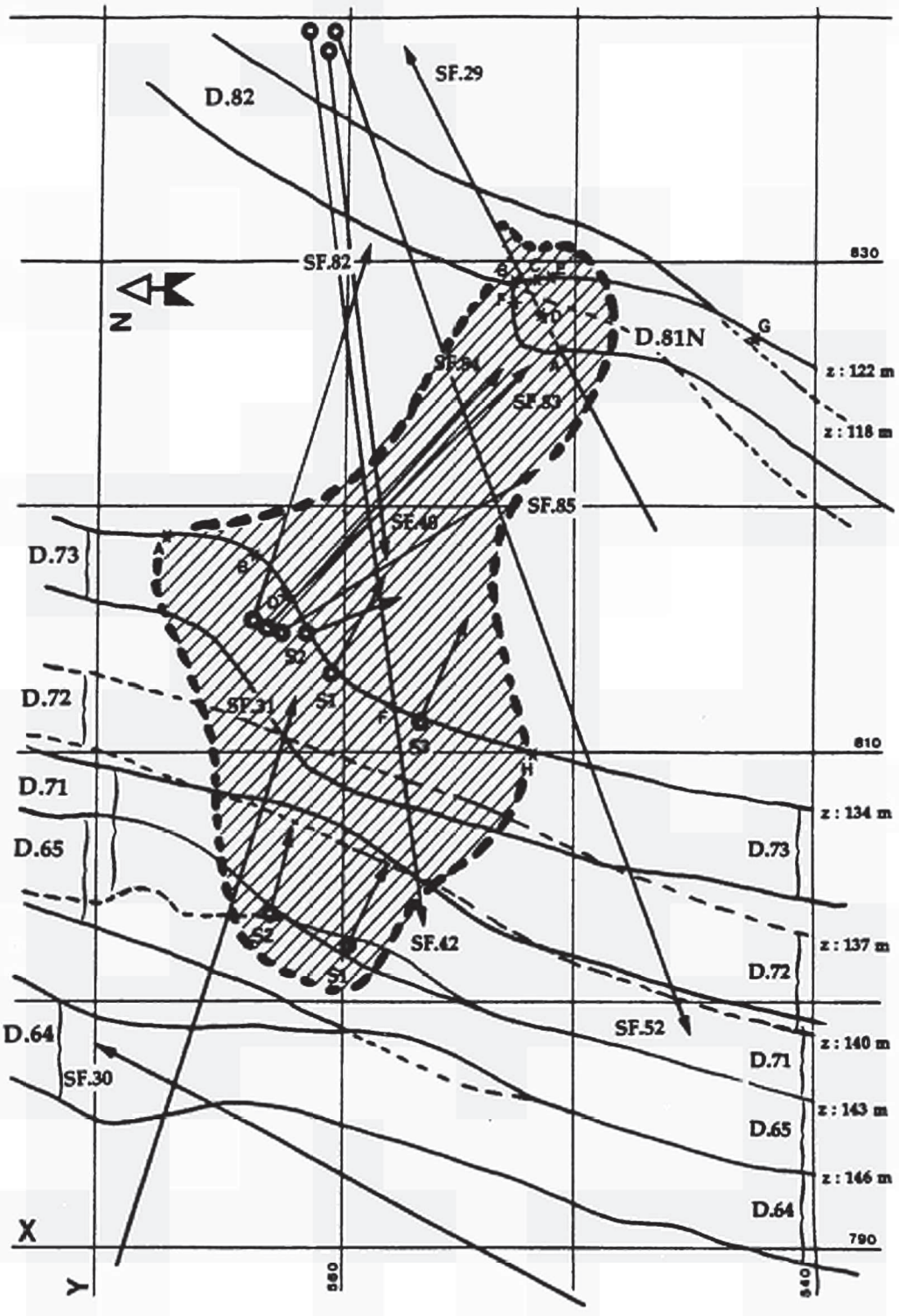
D.82
SF.29
SF.82
N
830
D.81N
G
z : 122 m
z : 118 m
SF.84
SF.83
SF.85
SF.48
D.73
D.72
SF.31
810
D.71
D.65
z : 134 m
D.73
z : 137 m
D.72
SF.42
SF.52
z : 140 m
D.71
z : 143 m
D.65
z : 146 m
D.64
SF.30
790
X
Y
860
840

FIGURE 1

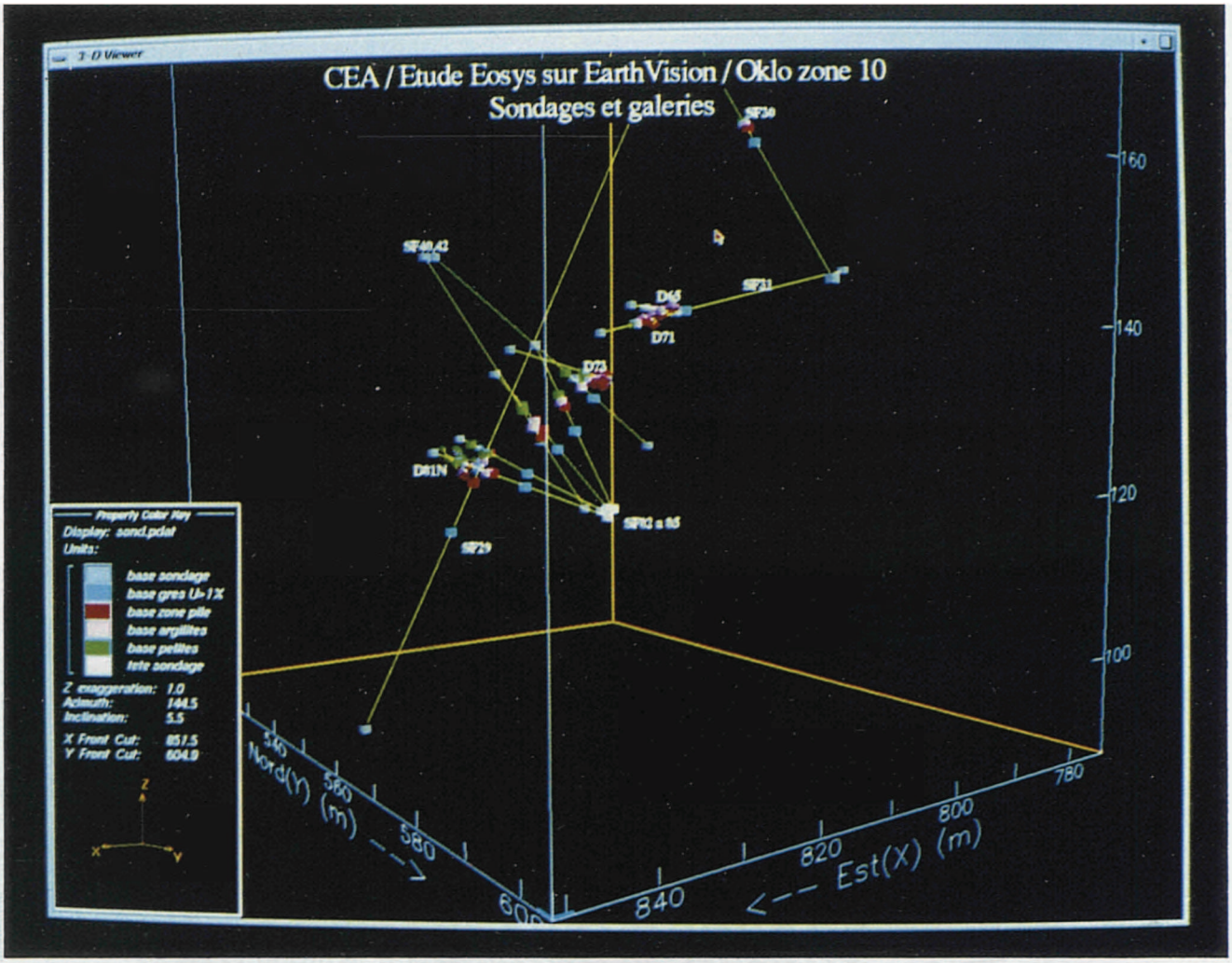

FIGURE 2

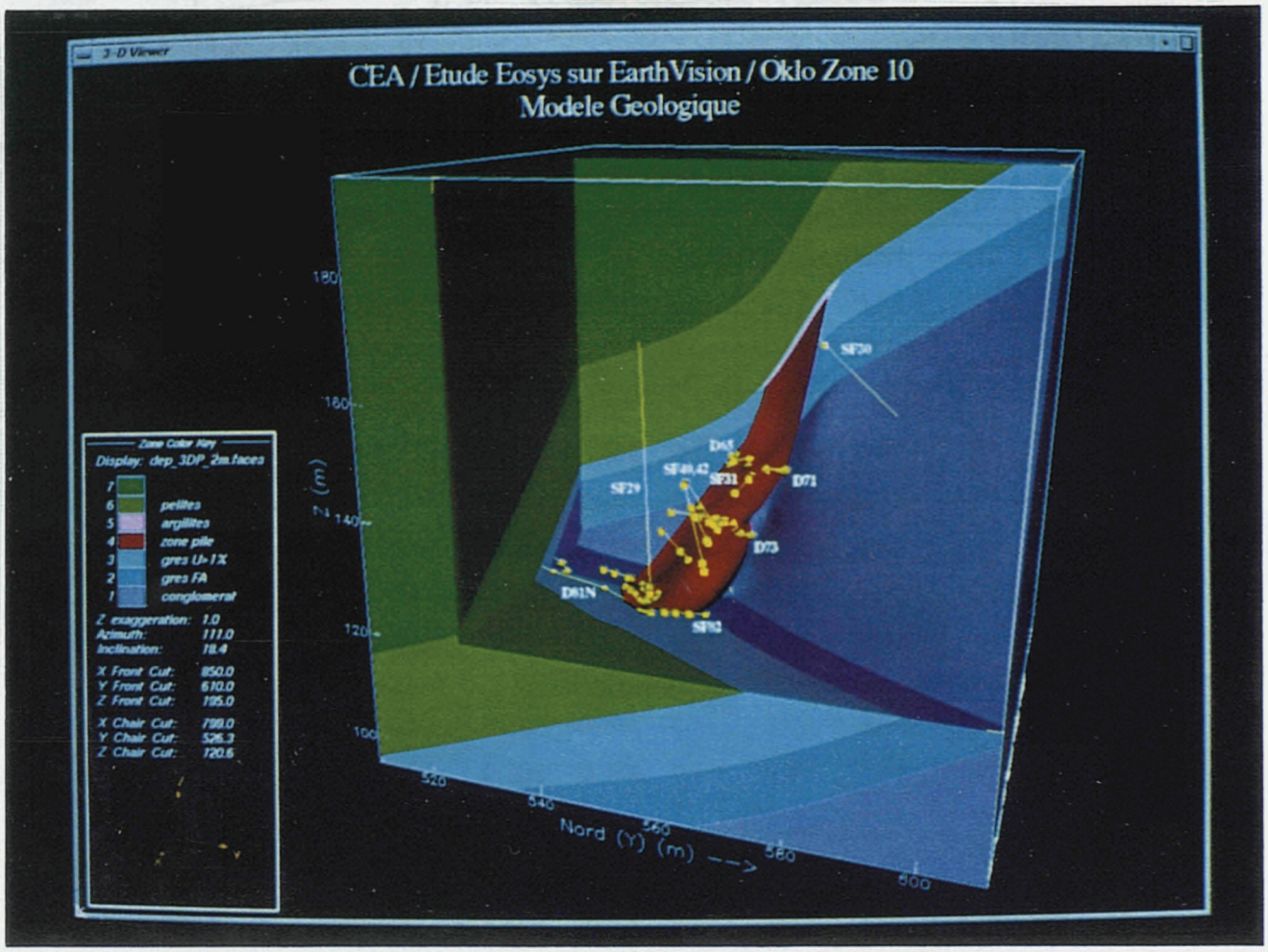

FIGURE 3

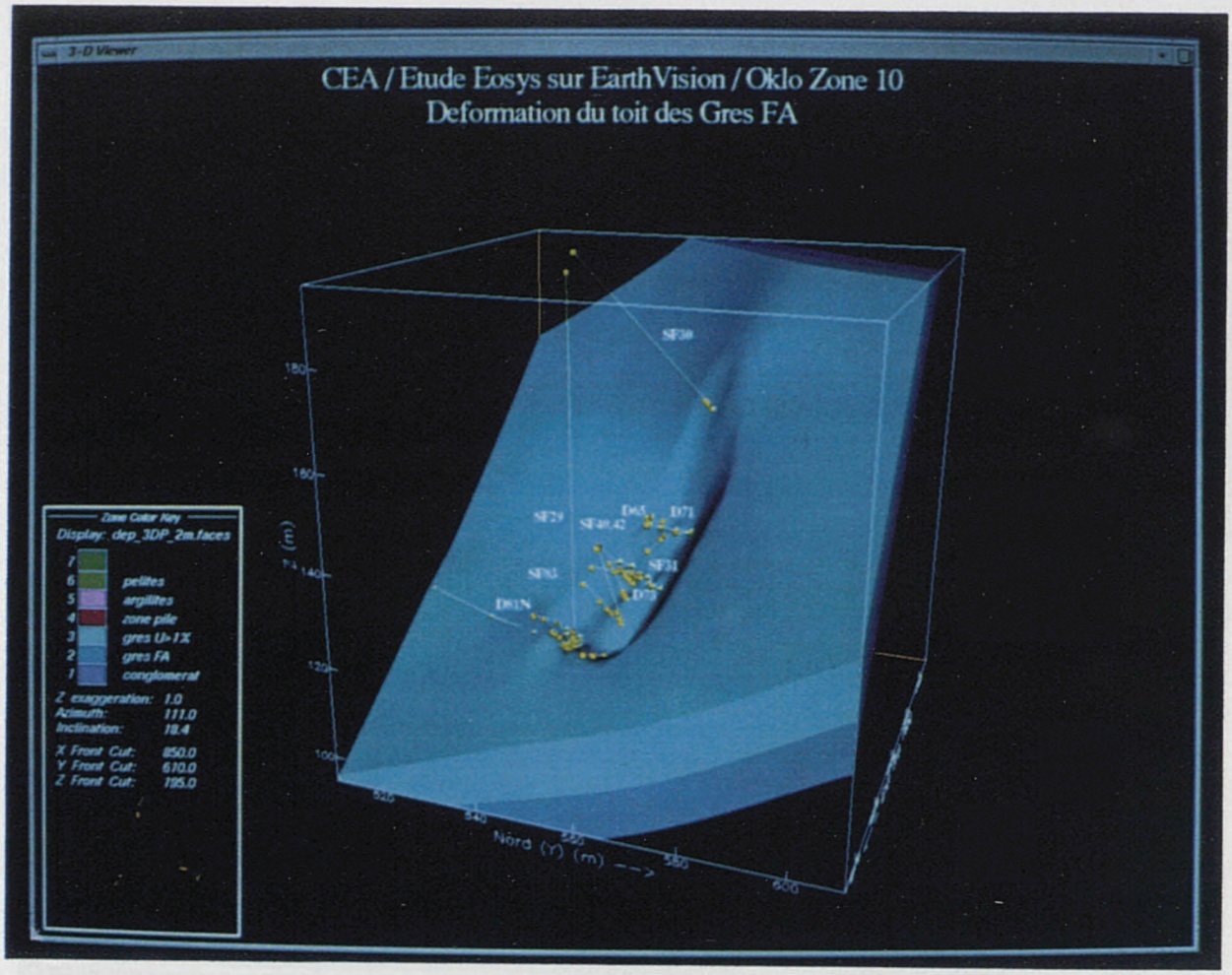

FIGURE 4

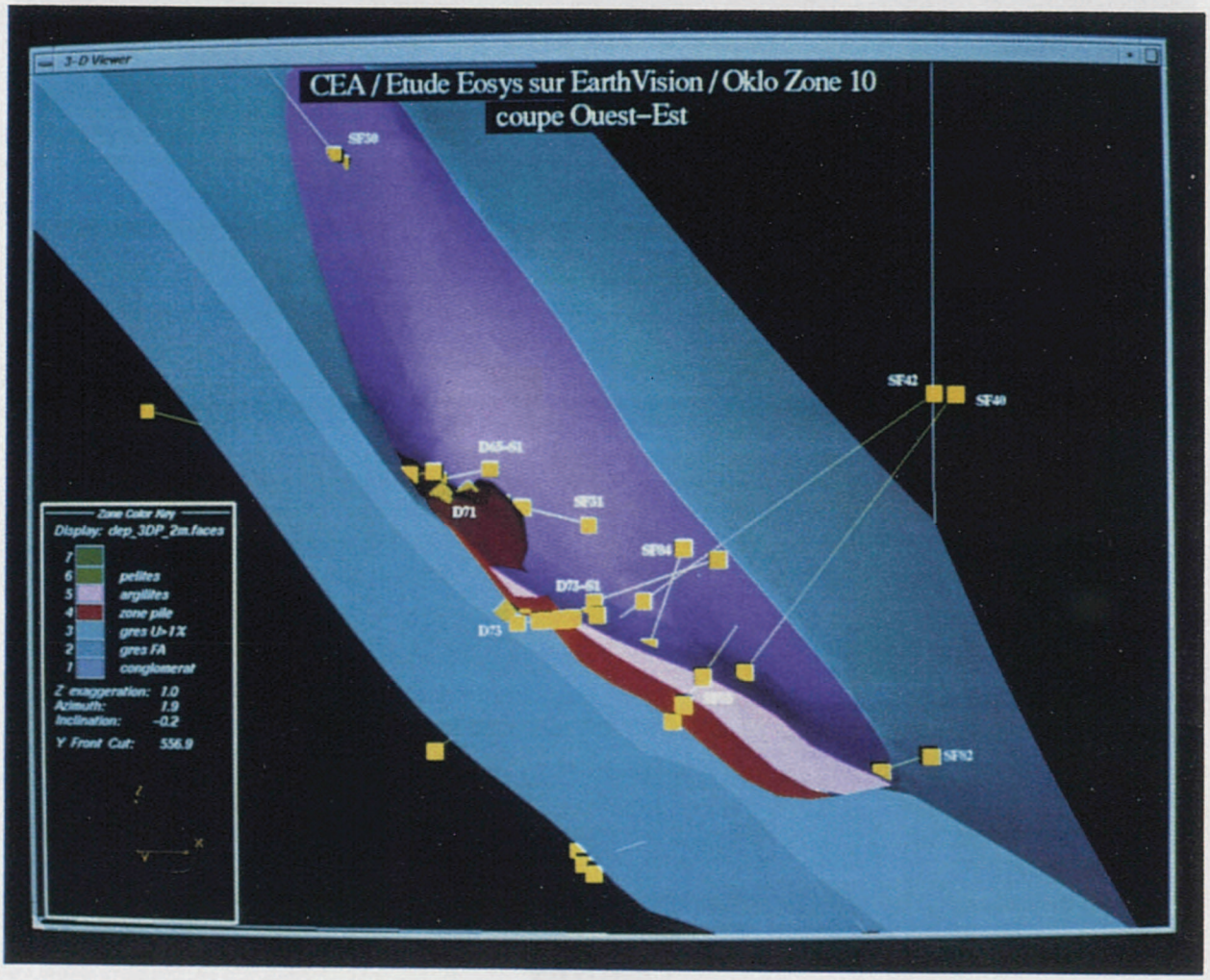

FIGURE 5

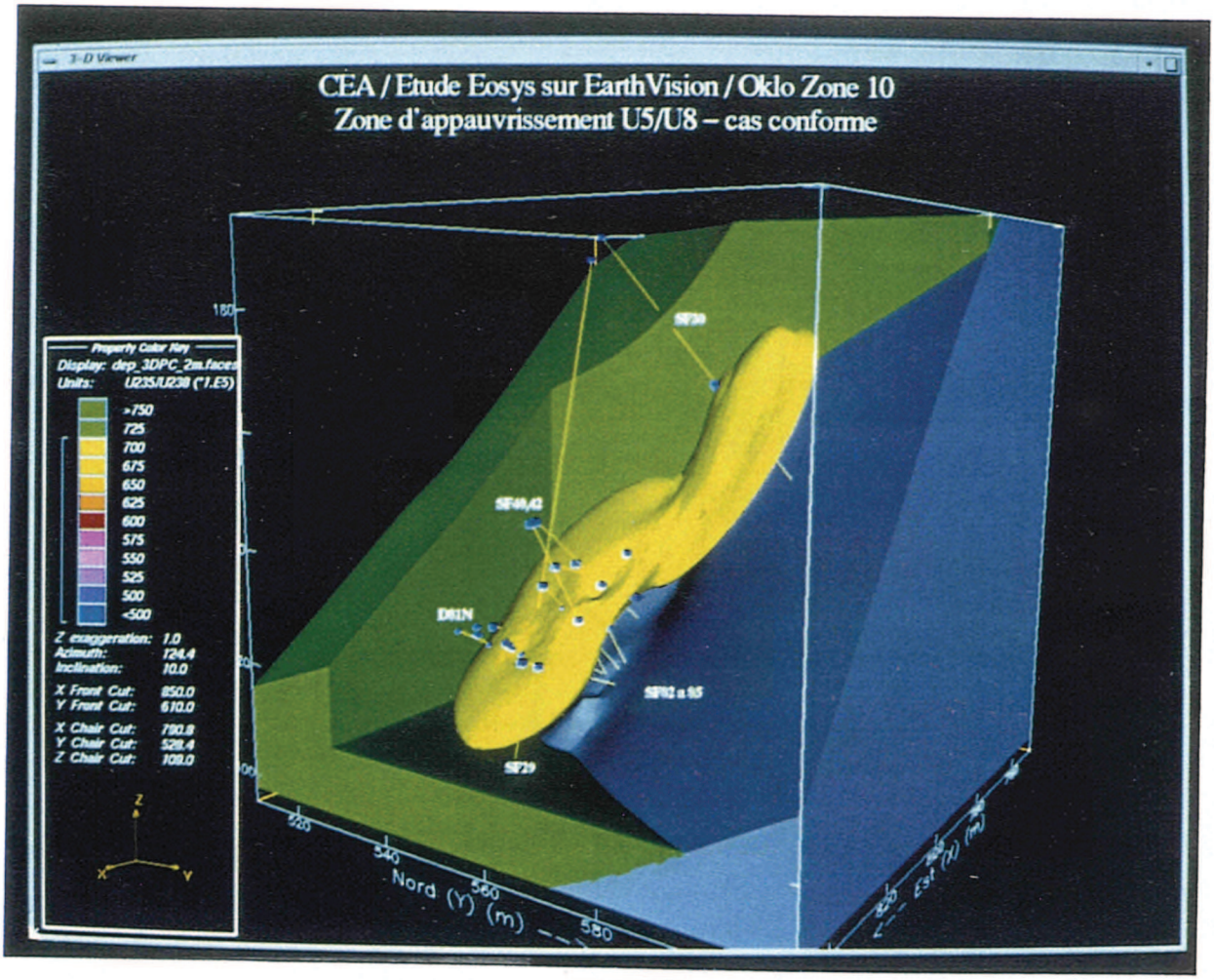

FIGURE 6

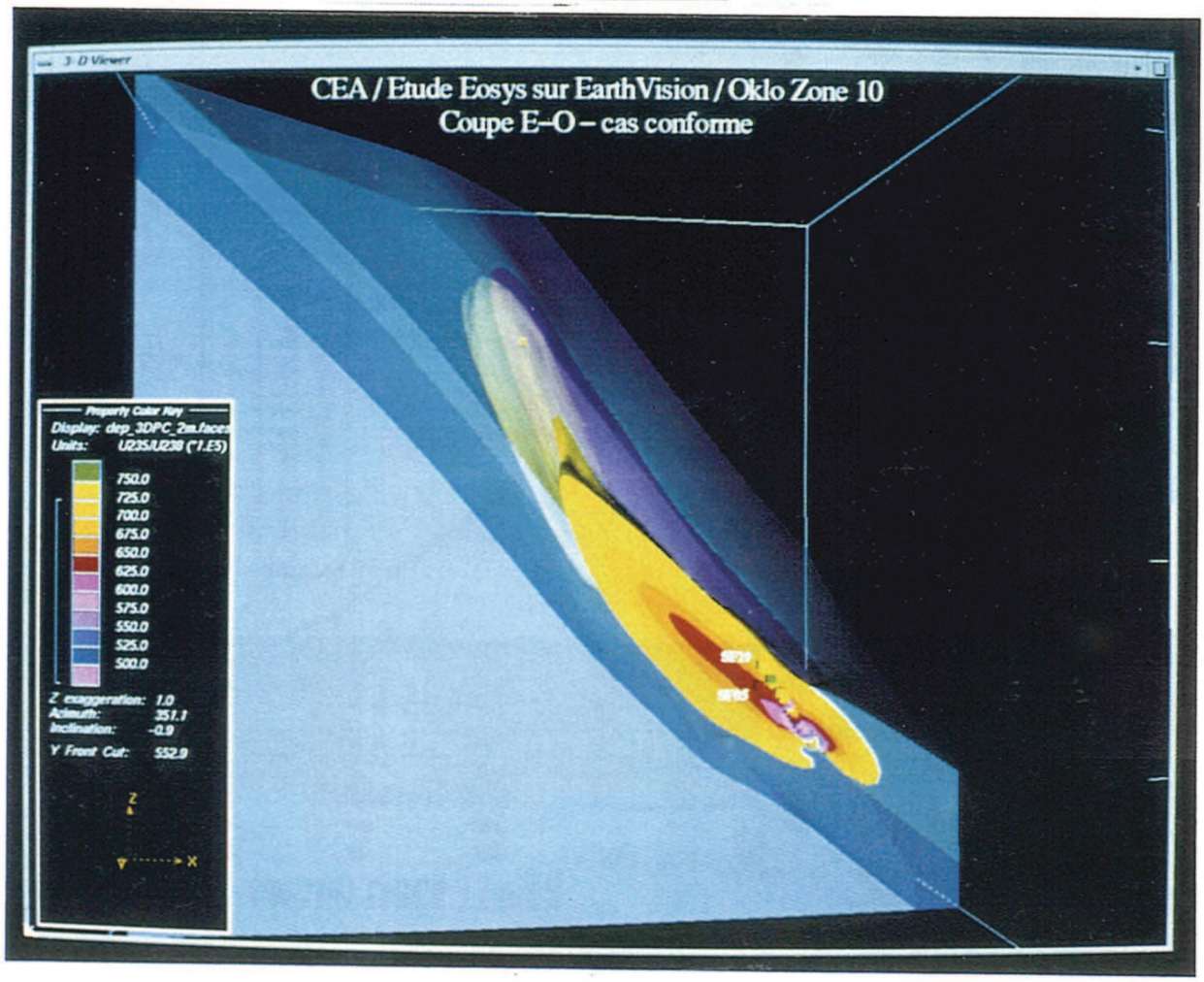

FIGURE 7

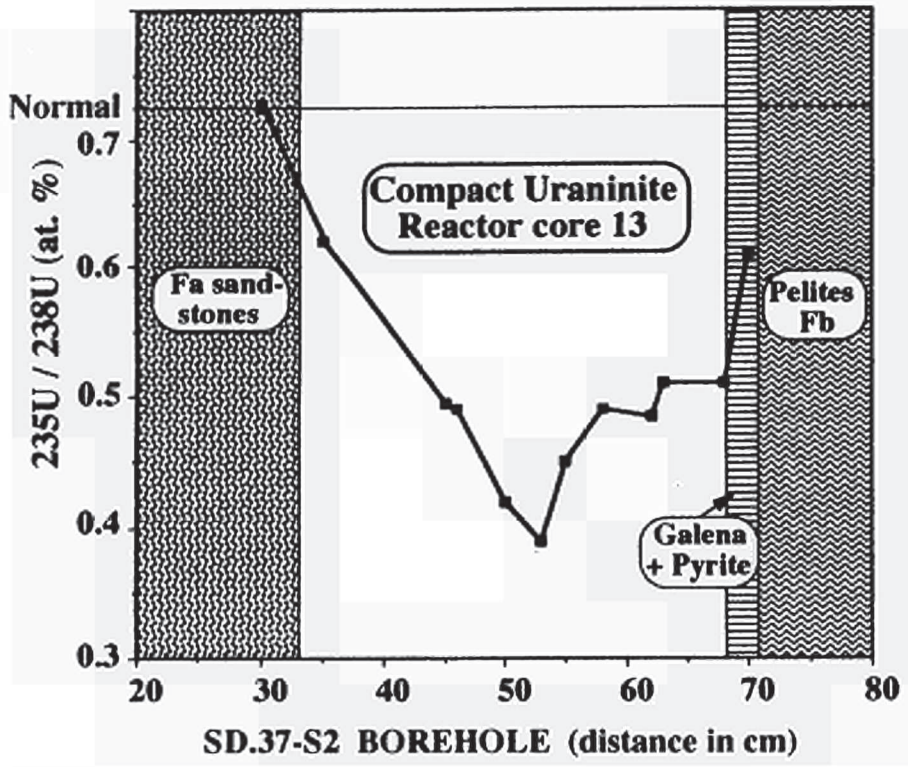

FIGURE 8

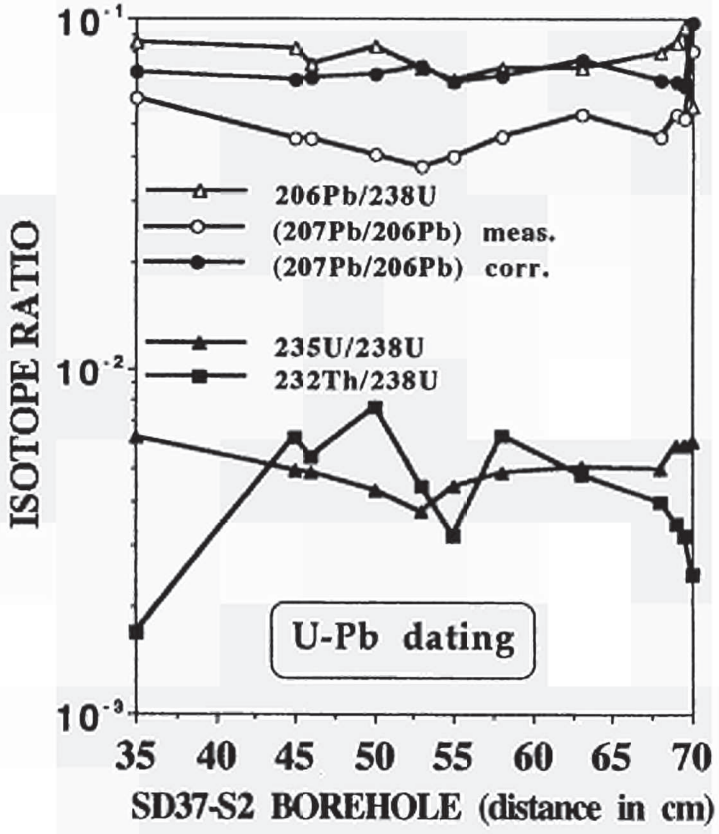

FIGURE 9

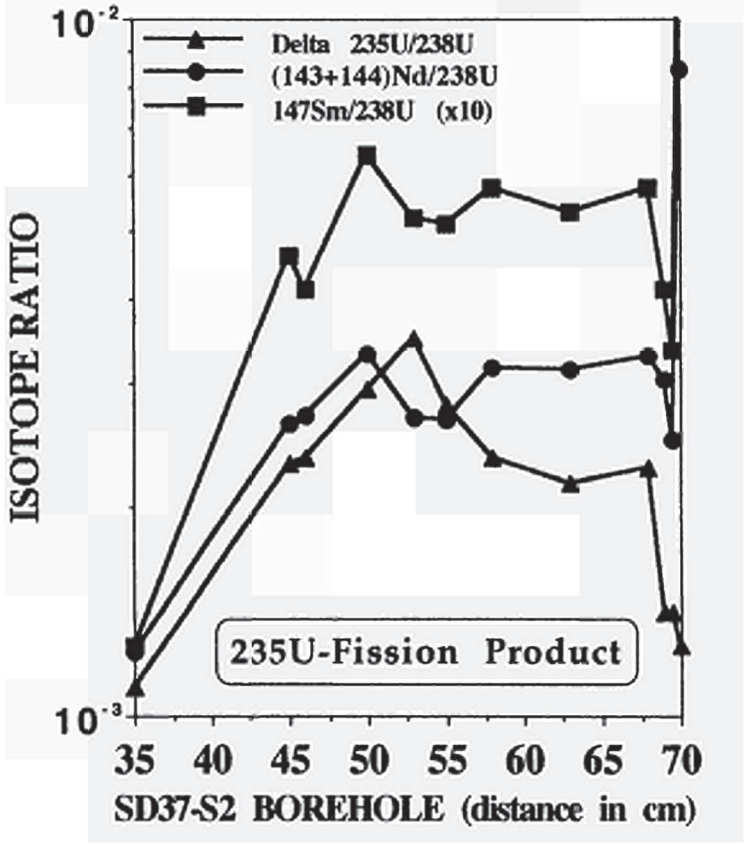

FIGURE 10

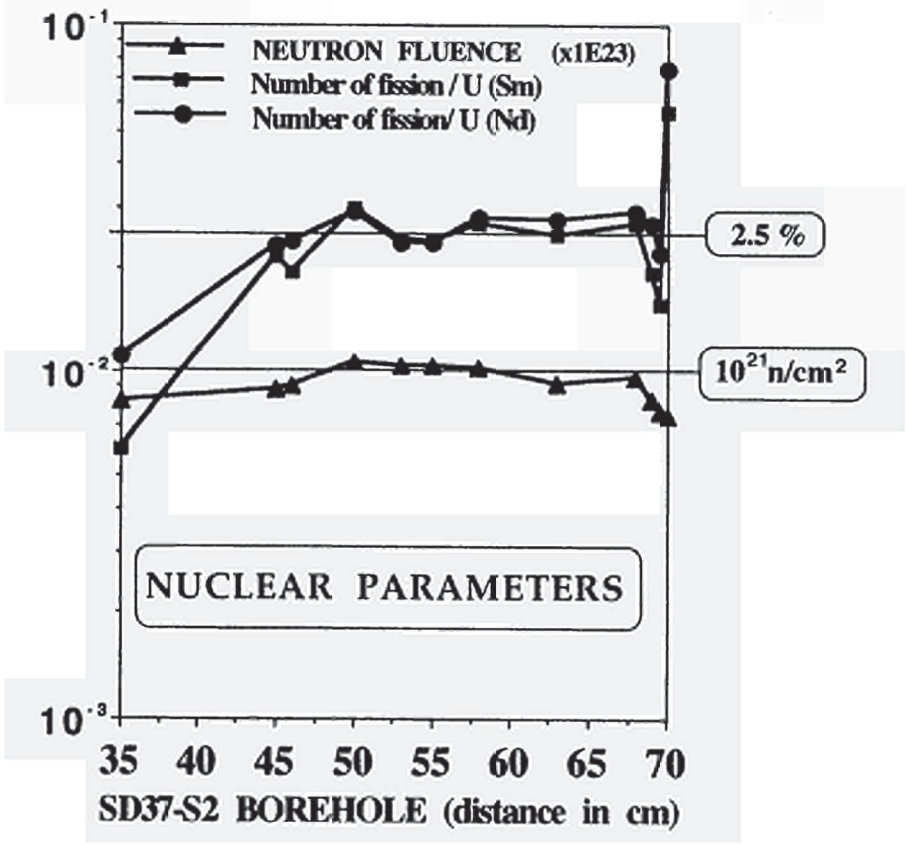

FIGURE 11

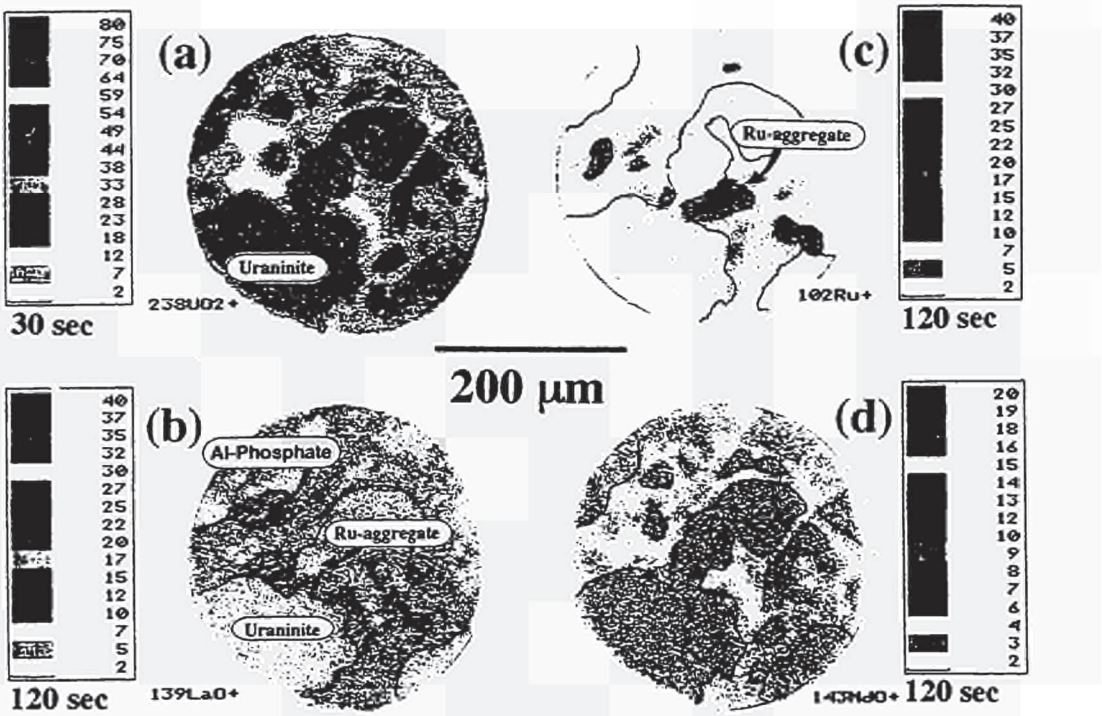

FIGURE 12

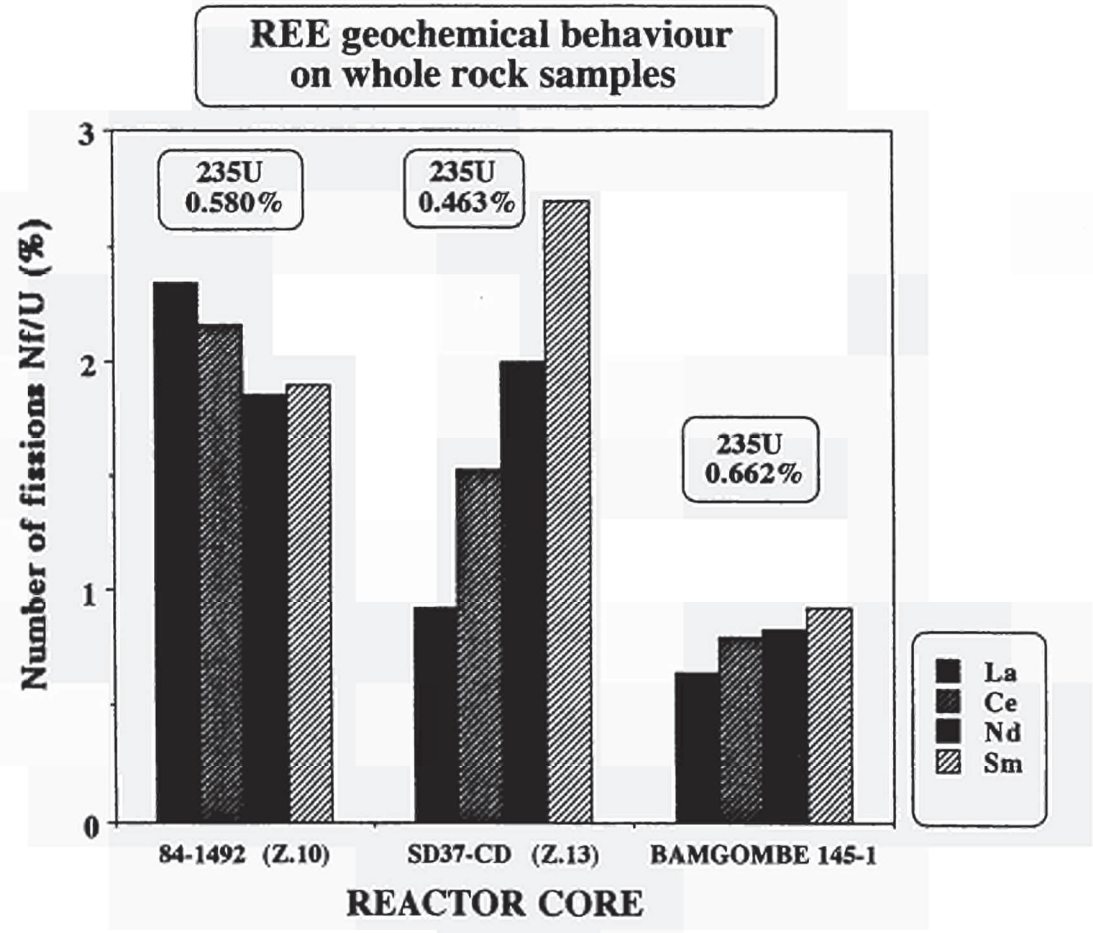

FIGURE 13